Journal of Materials Chemistry B

Materials for biology and medicine

www.rsc.org/MaterialsB

Volume 1 | Number 27 | 21 July 2013 | Pages 3333–3430

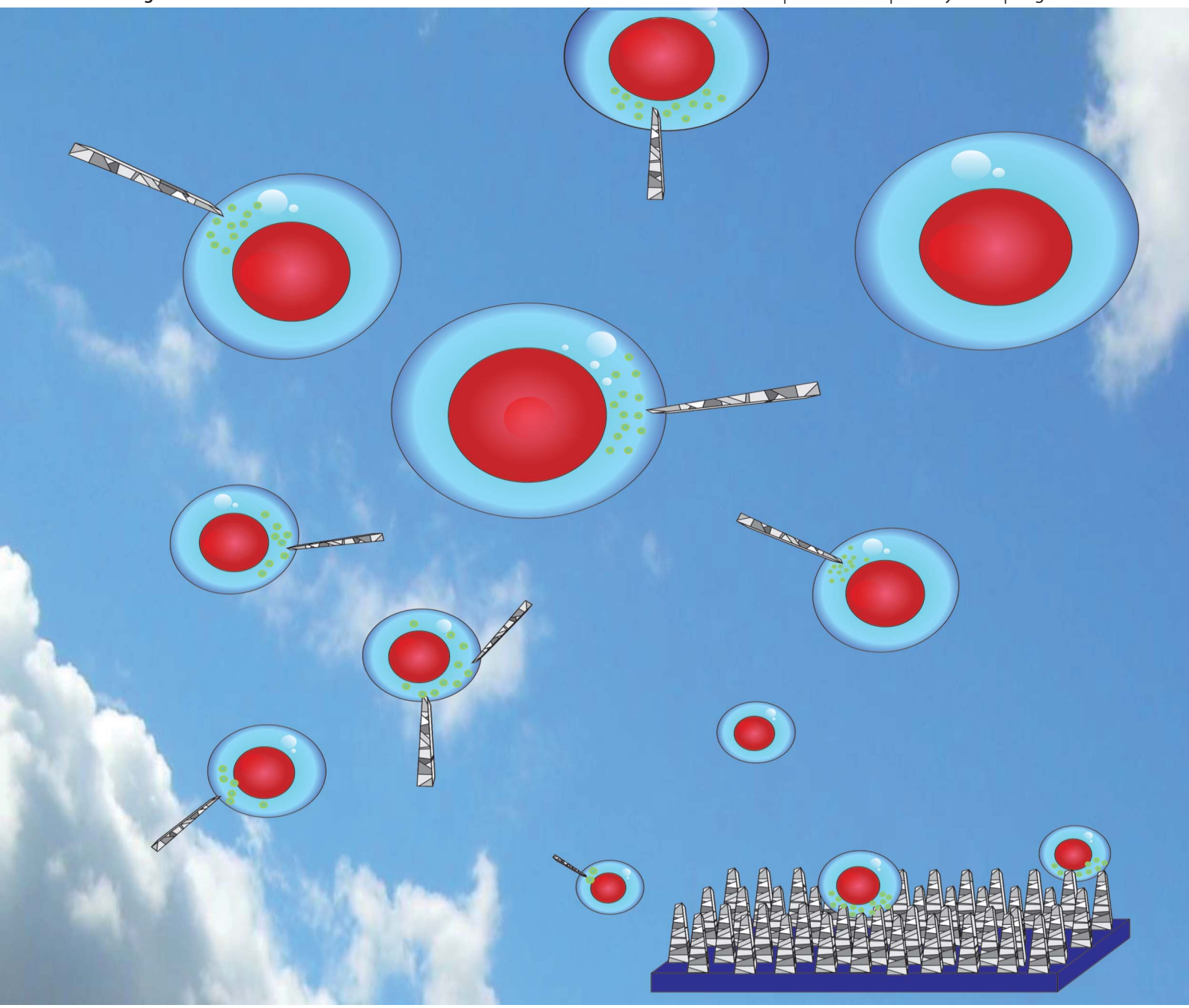

ISSN 2050-750X

RSC Publishing

PAPER

X. F. Chen, K. N. Yu *et al.*

A diamond nanocone array for improved osteoblastic differentiation

Journal of Materials Chemistry B

RSC Publishing

PAPER

A diamond nanocone array for improved osteoblastic differentiation†

Cite this: *J. Mater. Chem. B*, 2013, **1**, 3390

E. Y. W. Chong,‡[ab] C. Y. P. Ng,‡[a] V. W. Y. Choi,‡[a] L. Yan,[ac] Y. Yang,[ac] W. J. Zhang,[ac] K. W. K. Yeung,[b] X. F. Chen*[ac] and K. N. Yu*[a]

Received 25th January 2013
Accepted 20th May 2013

DOI: 10.1039/c3tb20114g

www.rsc.org/MaterialsB

Efficient delivery of biomolecules to cells is of great importance in biology and medicine. To achieve this, we designed a novel type of densely packed diamond nanocone array to conveniently transport molecules to the cytoplasm of a great number of cells. The nanocone array was fabricated by depositing a thin layer of diamond film on a silicon substrate followed by bias-assisted reactive ion etching. The height of the diamond nanocones varied from 200 nm to 1 μm with tip radii of approximately 10 nm. Our fluorescein and propidium iodide staining results clearly demonstrated that dramatically enhanced delivery of fluorescein into cells was realized without leading to noticeable cell death with the aid of nanocone treatment. As a test case of the drug delivery application of the device, MC-3T3 cells in differentiation medium were applied to the nanocone array for enhanced intracellular delivery of the medium. This was confirmed by the fact that nanocone treated cells experienced much higher differentiation ability at an early stage in comparison with untreated cells. Overall, the results indicate that the diamond nanocone array provides a very simple but yet very effective approach to achieve delivery of molecules to a large number of cells.

1 Introduction

Intracellular delivery through direct interfacing nanomaterials with cells is an attractive concept due to its simple procedures. In a pioneering study, Kim *et al.*[1] demonstrated that mammalian cells could be cultured on vertically aligned silicon nanowire (SiNW) array substrates, with the SiNW array naturally penetrating into the cells during incubation. In one test, HEK 293T cells were cultured on such a SiNW array with plasmid GFP DNA pre-deposited on the surface of the SiNWs and the result clearly showed GFP expression, indicating successful delivery and normal function of the exogenous gene.[1] With such a success, Shalek *et al.*[2] further demonstrated that surface-modified vertical silicon nanowires could form a generalized platform for introducing a diverse range of biomolecules into living cells. However, in these approaches, since cells need to be cultured as a monolayer on the nanowires, the number of cells will be limited by the surface area of the nanowire substrate. Furthermore, the cell culturing on nanowires takes a relatively long period of time and therefore the efficiency of intracellular delivery is low. In the present work, we explored further to enhance the efficiency and shorten the time required for drug delivery. Instead of relying on culturing cells to passively subside on the nanowires and allow the penetration of the nanowires, we actively applied cells to a nanocone array patch. With a low height and choice of diamond material, these nanocones are expected to be robust enough to breach cell membranes although their tip radii are extremely small (~10 nm). We proposed that such a device will aid the delivery of molecules into cells without causing irreversible damage to cells.

To test our hypothesis, we investigated whether the nanocone array could facilitate the delivery of differentiation medium to pre-osteoblasts which are of great importance in bone remodelling. Bone remodelling involves new bone formation and plays a significant role in bone fracture healing.[3,4] Osteoblasts, which are from mesenchymal precursor cells, are the cells responsible for the synthesis of the bone matrix.[5] Therefore, osteoblastic differentiation is a particular key step in bone formation. Tremendous efforts have been made to study factors affecting osteoblastic differentiation (*e.g.*, ref. 6). Enhancing early osteoblastic differentiation can help *in vitro* or *ex vivo* tissue engineering where cells are manipulated *in vitro* prior to implantation into the *in vivo* environment.[7–9] Different genes are expressed during cellular differentiation.[10] In the present work, we demonstrated the effectiveness of using a diamond nanocone

[a]*Department of Physics and Materials Science, City University of Hong Kong, Tat Chee Avenue, Kowloon Tong, Hong Kong, P.R. China. E-mail: peter.yu@cityu.edu.hk; xianfeng.chen@cityu.edu.hk; Fax: +852-34420538; Tel: +852-34427812*

[b]*Department of Orthopaedics and Traumatology, The University of Hong Kong, Pokfulam Road, Hong Kong, P.R. China*

[c]*Center of Super-Diamond and Advanced Films (COSDAF), City University of Hong Kong, Tat Chee Avenue, Kowloon Tong, Hong Kong, P.R. China*

† Electronic supplementary information (ESI) available. See DOI: 10.1039/c3tb20114g

‡ These authors contributed equally.

This journal is © The Royal Society of Chemistry 2013

array for significantly promoted early osteoblastic differentiation. The diamond nanocones enjoyed sufficient rigidity to be mechanically manipulated even with extremely small geometry. Importantly, different from the previous culturing cells on nanowires for intracellular delivery, our method is simple and convenient for a very high number of cells.

2 Methodology

2.1 Substrate fabrication

The diamond nanocone array was fabricated in an ASTeX® microwave plasma CVD reactor equipped with a 1.5 kW microwave generator. Pyramidal-shaped [001]-textured diamond films were first deposited on a (001) silicon wafer using bias-enhanced nucleation and maintaining the alpha growth parameters close to 3.[11] Subsequently, an *in situ* bias-assisted reactive ion etching process was applied. During the process, hydrogen was transferred to the microwave reactor at a gas flow rate of 200 sccm to maintain the reactant pressure at 40 Torr. The input microwave power and substrate temperature were 1500 W and 850 °C, respectively. A negative substrate bias of −400 V was applied to the substrates throughout the etching process, inducing a bias current of 140 mA. The etching process lasted for 40 min to form the diamond nanocone array. The diamond nanocone array was sterilized by 70% ethanol for at least 30 min before the start of the experiments. The array was then washed with PBS (phosphate-buffered saline) three times to remove all ethanol.

2.2 Cell culture

Mouse MC3T3-E1 pre-osteoblasts, which can differentiate into osteoblasts, were used in the present study. The cells were cultured at 37 °C with 5% carbon dioxide (CO_2) and 95% humidified air in Dulbecco's Modified Eagle Medium (DMEM) (Gibco) supplemented with 10% fetal bovine serum (FBS) (Gibco). The medium was renewed every 2–3 days and confluent cells were subcultured through trypsinization.

2.3 Intracellular delivery

Before the intracellular delivery study, the potential effect of nanocone treatment on the viability and morphology of MC-3T3 cells was investigated by a methyl thiazolyl tetrazolium (MTT) assay and optical microscopy, respectively. Three groups of cells were studied. One group was untreated cells. Other two groups included the cells that were treated by the smooth silicon substrate and the diamond nanocone array. For treatment, a volume of 1 ml of MC-3T3 cell suspension was applied to the substrate with a speed of about 3 m s^{-1} using a pipette. After the application, the cell suspension was collected and pipetted to the substrate again with a similar speed. Such a cell treatment procedure was repeated 15 times. The same procedures were used in all experiments for enhanced intracellular delivery. Following cell treatment, cells were plated into 96-well microtiter plates. After 22 hours, the morphology of each group of cells was observed by optical microscopy. After 24 hours, cell viability was determined by the MTT assay.

Subsequently, the enhanced intracellular delivery capability of the diamond nanocone array was first assessed by investigating the fluorescence intensity of fluorescein sodium salt stain in treated cells by quantitative analysis through flow cytometry. MC-3T3 cells were harvested at a density of 10^4 cells per ml. Fluorescein was added to cell growth medium at a concentration of 1 mg ml^{-1}. After the addition of fluorescein, a volume of 1 ml of this cell suspension was treated with the same method as that described above. Two experiments were arranged in investigating the intracellular delivery of fluorescein sodium salt. In one experiment, the negative control was to apply cells to a smooth silicon substrate without the nanocone array. In the other experiment, untreated cells were used as the control (*i.e.*, neither a nanocone array nor a smooth Si substrate was used). After 15 min staining, the suspensions of control and treated group cells were pelleted by centrifugation (Spectrafuge™ 16M, Labnet) at 6000 rpm for 3 min, after which the supernatants were removed. The cell pellets were washed with 1 ml of phosphate buffered saline (PBS) and then resuspended thoroughly. The cell suspensions were centrifuged again at 6000 rpm for 3 min, and the cell pellets were washed with PBS 3 times in total. Finally, the cell suspensions were prepared with a concentration of 10^4 cells in PBS and then they were immediately analysed using a flow cytometer (Becton DICKINSON, FACSCalibur cytometer) by counting 1×10^4 cells per sample. For blank analysis during flow cytometry, a cell suspension with a concentration of 10^4 cells without fluorescein staining was also prepared.

The diamond nanocone array was further tested for the prompted delivery of the differentiation agent to osteoblast cells. MC-3T3 cells were harvested at a density of 2.5×10^4 cells per ml. Cell differentiation was induced by adding 50 μg ml^{-1} ascorbic acid (Sigma, USA) and 20 mM β-glycerol phosphate (Sigma, USA) to the growth medium (named as "differentiation medium"). A volume of 1 ml of this cell suspension, containing 2.5×10^4 MC-3T3 cells, was treated by a nanocone array patch in the same way as that used in fluorescein delivery. The treated cells were then transferred to 24-well plates. A total of 5 to 8 wells were filled with the treated cells in 1 ml of differentiation medium (*i.e.*, $N = 5$ or 8, respectively) (see Fig. 1). At the same time, the same number of wells with untreated cells with the same cell concentration were prepared and used as controls. The differentiation medium was replaced every 2 to 3 days and measurements were made on the 3^{rd}, 7^{th} and 14^{th} days.

2.4 Cell differentiation

At designated time points, *i.e.*, on the 3^{rd}, 7^{th} and 14^{th} days, the cells were lysed using 100 μl of lysis buffer (0.1% Triton X-100 in PBS) for 10 min at 4 °C with gentle rocking. The lysate in each well was then separately transferred to different Eppendorfs. To separate the cell protein and debris, the lysate was centrifuged at 4 °C with a speed of 300 rpm for 10 min. The alkaline phosphatase (ALP) activity and the protein level of the supernatant were then determined.

Total protein level. The cell protein content was measured by using protein dye (Bio-Rad), which was warmed to 37 °C before use. A volume of 10 μl of cell lysate for each sample was

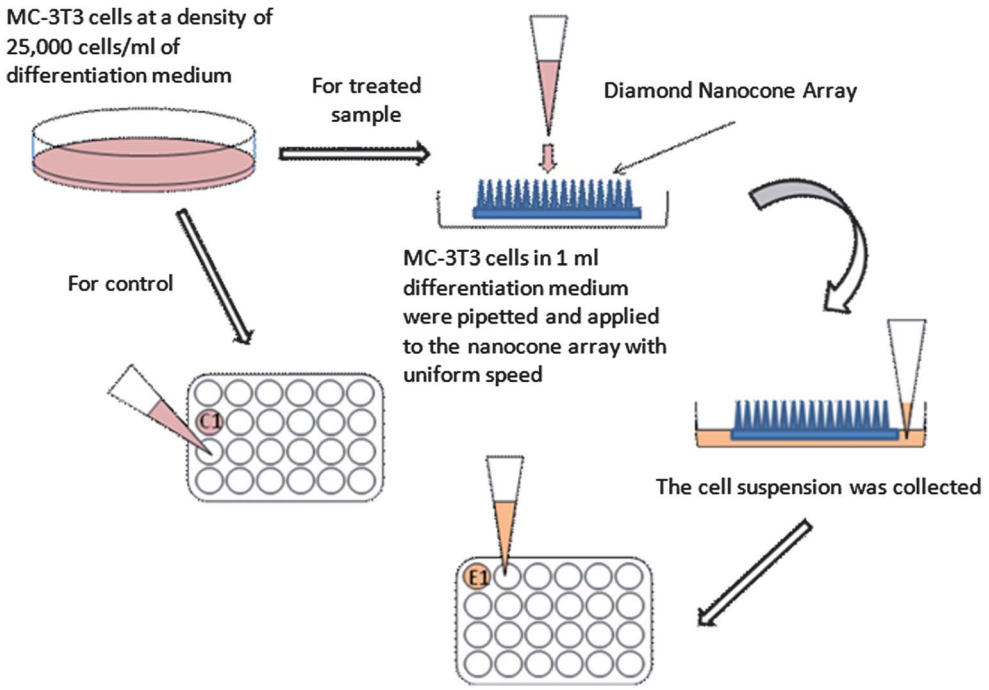

Fig. 1 Schematic diagram showing the cell treatment procedure.

transferred to a 96-well plate, and then 200 μl of protein dye was added to each well. Furthermore, 10 μl of bovine serum albumin (BSA) at 6 different concentrations (0.50, 0.25, 0.125, 0.0625, 0.03125 and 0 mg ml^{-1}) were used to obtain a standard curve. The optical densities at 595 nm were measured with a UV-Vis-IR Microplate Reader (Powerwave XS MQX200R). An average cellular protein level for each cell sample was recorded.

Alkaline phosphatase (ALP) activity. The alkaline phosphatase (ALP) activity, one of the typical markers for osteoblastic differentiation, was studied with an alkaline phosphatase activity assay kit (Stanbio Alkaline Phosphatase LiquiColor®). Alkaline phosphatase buffer and the alkaline phosphatase substrate were mixed in a ratio of 5 : 1 and the mixture was warmed to 37 °C. A volume of 10 μl of the supernatant from each Eppendorf prepared above was transferred to a 96-well plate. The 96-well plate with all supernatant to be measured was pre-warmed to 37 °C before adding 200 μl of ALP indicator to each well. The absorbance at 405 nm was measured using a UV-Vis-IR Microplate Reader (Powerwave XS MQX200R) immediately in the dark and was consecutively recorded every 1 min for a total of 4 min at 37 °C. The enzymatic activity was normalized to the total protein concentration. An average normalized ALP level was then obtained for each cell sample.

Data analysis. The experiments were repeated 3 to 5 times for measurements on different days. For each set of experiments, the ALP levels A_C and A_T for the control group and the treated group were measured. Since the normalized ALP levels on the control samples could vary for different sets of experiments, in order to combine all the data, we first transformed the data to $A_C^* = [A_C - \langle A_C \rangle]/\langle A_C \rangle$, where $\langle A_C \rangle$ is the average ALP level for a control group in a particular set of experiments, and similarly the normalized net ALP levels in the treated samples as $A_T^* = [A_T - \langle A_C \rangle]/\langle A_C \rangle$. The distributions of A_C^* and A_T^* were compared using the two-sample Kolmogorov–Smirnov test (2-tailed).

Furthermore, the mean values of A_T^* and A_C^* were compared through the non-parametric Mann–Whitney U test (2-tailed). Cases with $p < 0.05$ were considered as statistically significant.

3 Results

3.1 Diamond nanocones

Fig. 2 shows the SEM images of a diamond nanocone array. The nanocones were highly densely packed. The heights varied from 200 nm to 1 μm. The tip radius of the nanocones is mostly below 10 nm. The density of the nanocones is over 10^9 per cm^2.

3.2 Effect of treatment on cell morphology and viability

Fig. 3 shows the optical microscopy images of three groups of cells. Fig. 3A and B show cells which were applied to a diamond

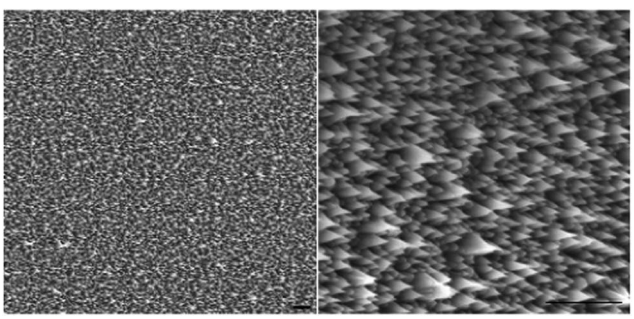

Fig. 2 SEM images of a diamond nanocone array. (The scale bars indicate 1 μm.)

This journal is © The Royal Society of Chemistry 2013

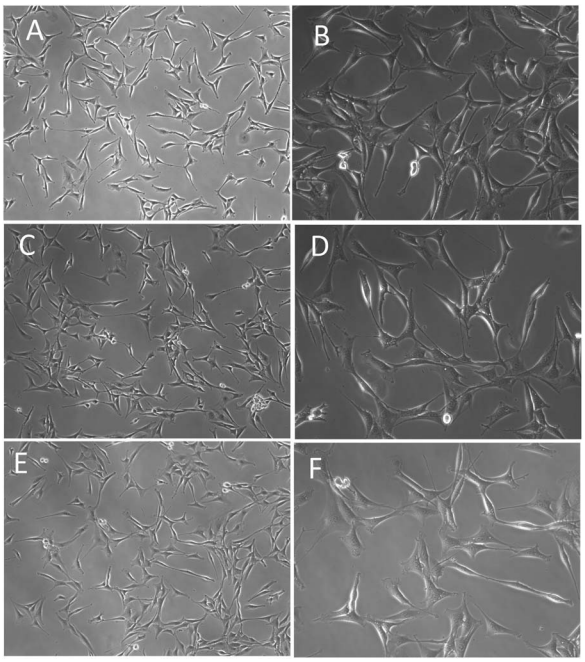

Fig. 3 Optical microscopy images (magnifications of 10× (A, C and E) and 20× (B, D and F)) of diamond nanocone treated cells (A and B), smooth silicon substrate treated cells (C and D) and untreated cells (E and F).

nanocone array and then plated to a 96-well plate. Fig. 3C and D show smooth silicon substrate treated cells while untreated cells are shown in Fig. 3E and F. These images clearly reveal that the cell morphology was not affected by either diamond nanocone or smooth silicon substrate treatment.

Fig. 4 displays the viability of cells with and without treatment. The same three groups (untreated cells, cells treated by either a diamond nanocone or a smooth silicon substrate) were investigated. The results indicate that both the treatment methods, most importantly, diamond nanocone treatment did not cause noticeable cell death. This is very important in using the technology for enhanced intracellular delivery.

3.3 Intracellular delivery

After confirming that both cell morphology and viability were not negatively affected by diamond nanocone treatment, the enhanced intracellular delivery was quantitatively assessed through flow cytometry. Two experiments were arranged with the same parameters (*e.g.*, concentration of cells and fluorescein sodium salt) in investigating the intracellular delivery of fluorescein sodium salt. In one experiment, untreated cells were used as a negative control, while in the other experiment cells which were treated by a smooth Si substrate were used as a negative control. The results are shown in Fig. 5 and 6. The cell population was divided into four groups according to their fluorescence intensities. The percentages of cells exhibiting fluorescence intensities of 1×10^0 to 1×10^1, 1×10^1 to 1×10^2, 1×10^2 to 1×10^3 and 1×10^3 to 1×10^4 were denoted as M1, M2, M3 and M4, respectively, in each histogram. Fig. 5 shows that the fluorescence dominated in M2 (*viz.*, M2 = 63.1%) for the control sample, while the fluorescence dominated in M3 (*viz.*, M3 = 73.5%) for the cells treated with the nanocone array. These results quantitatively and unambiguously showed that many more treated cells exhibited stronger fluorescence, which proved enhanced intracellular delivery by the nanocone array. On the other hand, Fig. 6 shows that the fluorescence dominated in M2 (*viz.*, M2 = 70.0%) for the untreated sample, while the fluorescence dominated in M3 (*viz.*, M3 = 62.4%) again for

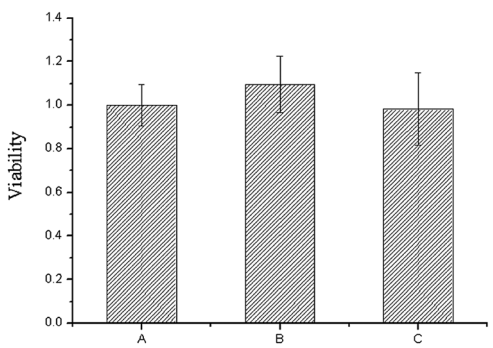

Fig. 4 Viability of cells which were not treated (A), treated by a smooth silicon substrate (B), and treated by a diamond nanocone array (C). Cell viability does not have statistical difference among groups ($p > 0.05$).

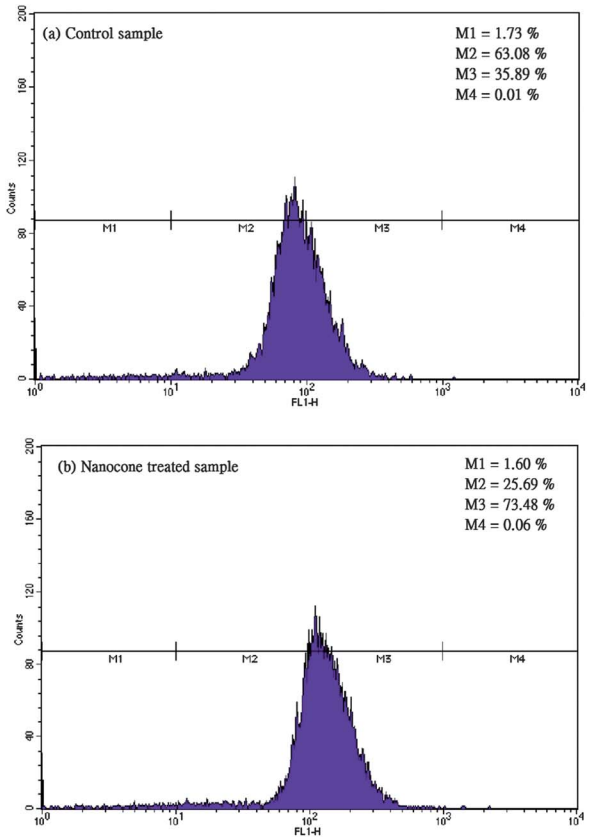

Fig. 5 Flow cytometry analysis of the fluorescence intensities of control and nanocone treated MC-3T3 cells. (a) Fluorescence histogram of a control sample. (b) Fluorescence histogram of the sample treated with the nanocone array. The *x*-axis plots FL-1 fluorescence intensity in the log scale; the *y*-axis gives the cell number. The percentages of cells exhibiting fluorescence intensities of 1×10^0 to 1×10^1, 1×10^1 to 1×10^2, 1×10^2 to 1×10^3 and 1×10^3 to 1×10^4 were denoted as M1, M2, M3 and M4, respectively, in each histogram.

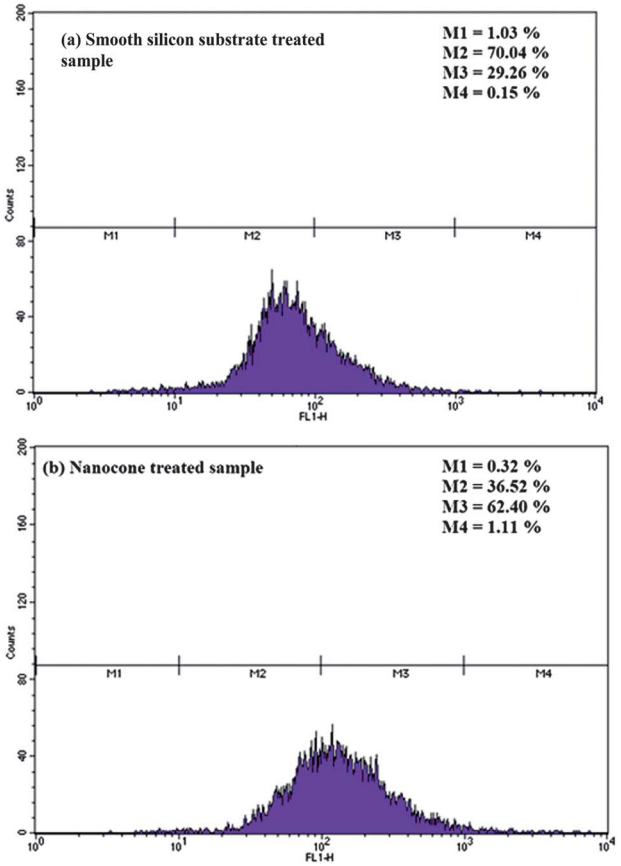

Fig. 6 Flow cytometry analysis of the fluorescence intensities of untreated and nanocone treated MC-3T3 cells. (a) Fluorescence histogram of an untreated sample. (b) Fluorescence histogram of the sample treated with the nanocone array. The *x*-axis plots FL-1 fluorescence intensity in the log scale; the *y*-axis gives the cell number. The percentages of cells exhibiting fluorescence intensities of 1×10^0 to 1×10^1, 1×10^1 to 1×10^2, 1×10^2 to 1×10^3 and 1×10^3 to 1×10^4 were denoted as M1, M2, M3 and M4, respectively, in each histogram.

the cells treated with the nanocone array. The data of the nanocone treated cells in the two experiments are comparable, which demonstrated the repeatability of the method. When comparing the flow cytometry data of the cells which were treated by a smooth Si substrate and the untreated cells, it was found that treatment by the smooth silicon substrate did not enhance the intracellular delivery when compared to the untreated cells.

Furthermore, propidium iodide staining showed that the cells treated with the present diamond nanocones and the control cells demonstrated similar viability, which is a particularly desirable feature of the nanocones.

3.4 Alkaline phosphatase activity (ALP activity)

The measurements made on the 3rd, 7th and 14th days were repeated 5, 4 and 3 times, respectively. The data for A_T^* and A_C^* for measurements made on the 3rd day denoted as $A_T^*(3)$ and $A_C^*(3)$, those for measurements made on the 7th day denoted as $A_T^*(7)$ and $A_C^*(7)$, and those for measurements made on the 14th day denoted as $A_T^*(14)$ and $A_C^*(14)$ are presented in Table 1 together with the associated information, including the total number of measurements (N), their means and standard errors (SE).

Table 1 Data for $A_T^*(3)$, $A_C^*(3)$, $A_T^*(7)$, $A_C^*(7)$, $A_T^*(14)$ and $A_C^*(14)$, including the total number of measurements (N), their means and standard errors (SE). The p values (2-tailed) between nanocone-array treated groups and controls for the two-sample Kolmogorov–Smirnov test, *i.e.*, p(K–S test), and that for the Mann–Whitney U test, *i.e.*, $p(U$ test), are also shown

	$A_T^*(3)$	$A_C^*(3)$	$A_T^*(7)$	$A_C^*(7)$	$A_T^*(14)$	$A_C^*(14)$
N	39	36	29	28	19	17
Mean	0.4681	0.0000	0.2541	0.0000	0.0124	0.0000
SE	0.0753	0.0300	0.0514	0.0312	0.0718	0.0298
p(K–S test)	0.000		0.000		0.594	
$p(U$ test)	0.000		0.001		0.381	

Fig. 7(a)–(c) show the distribution of the results on A_C^* and A_T^*, for measurements made on the 3rd, 7th and 14th days, respectively. It can be observed that the distributions for A_C^* and A_T^* are very different for the 3rd and 7th days, while they are relatively similar for the 14th day. In general, for the 3rd and 7th days, A_T^* peaks at larger values and spreads over larger ranges when compared to A_C^*. The distributions of A_T^* and A_C^* were compared through the two-sample Kolmogorov–Smirnov test (2-tailed). The p values are given in Table 1 as p(K–S test). The p values show that the distributions of A_T^* and A_C^* for measurements made on the 3rd and 7th days are significantly different, while those made on the 14th day are not significantly different.

On the other hand, the mean values of A_T^* and A_C^* were compared through the non-parametric Mann–Whitney U test (2-tailed). The p values are given in Table 1 as $p(U$ test). The p values show that the mean values of A_T^* and A_C^* for measurements made on the 3rd and 7th days are significantly different, while those made on the 14th day are not significantly different. From these results, we observed that the MC-3T3 cells that were pipetted down onto the nanocone array revealed significantly higher ALP activities on the 3rd and 7th days after treatment, when compared to the control samples, implying enhanced osteoblastic differentiation in the early period after treatment. On the other hand, we also observed that the treated cells did not show significantly higher ALP activities on the 14th day after treatment, implying no enhanced osteoblastic differentiation in the later period after treatment.

4 Discussion

In the present paper, we designed a highly densely packed nanocone array to mechanically disrupt cell membranes for enhanced delivery of drug molecules into a very high number of cells.

Diamond was selected to grow the nanocone array with such a small geometry because its significantly high Young's modulus ensured that these ultra-small nanocones are mechanically robust enough to breach cell membranes. Moreover, its intrinsic biocompatibility might minimize harmful effects to cells.

The nanocones were highly densely packed with a density over 10^9 per cm^2 and sizes in the nanometer range. They were

 This journal is © The Royal Society of Chemistry 2013

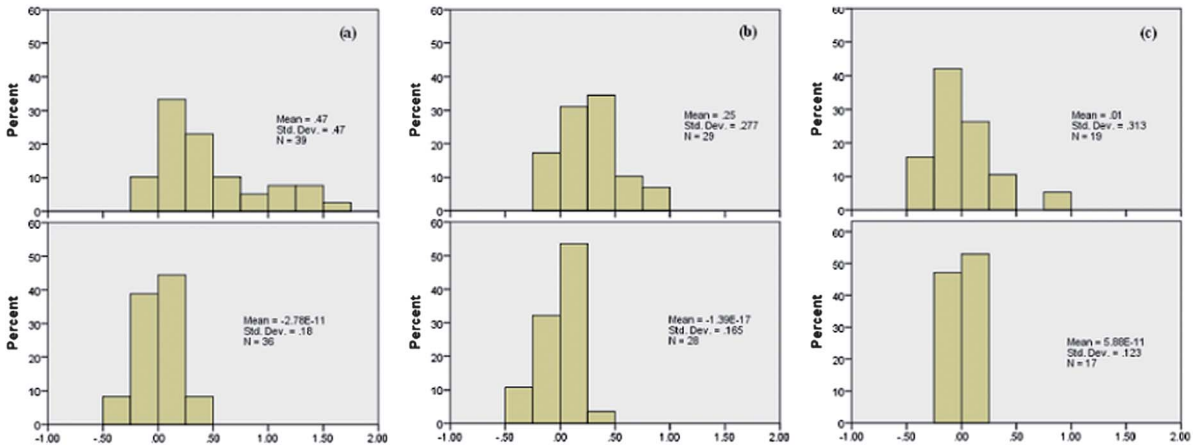

Fig. 7 Schematic distributions of A_T^* and A_C^* of measurements made on (a) the 3rd day, (b) the 7th day, and (c) the 14th day. Upper figures are for nanocone-array treated groups and lower figures are for the untreated control groups. For each set of experiments, the ALP levels A_C and A_T for the treated group and the control group were measured, and were then transformed to $A_T^* = [A_T - \langle A_C \rangle]/\langle A_C \rangle$ and $A_C^* = [A_C - \langle A_C \rangle]/\langle A_C \rangle$, where $\langle A_C \rangle$ was the average ALP level for a control group in a particular set of experiments. The right shift of the distribution in nanocone-array treated groups indicates faster differentiation of cells.

designed to mechanically disrupt cell membranes to enhance intracellular delivery of drug molecules without causing irreversible damage. The geometry and the aspect ratios of these diamond nanocones were significantly different from those of the nanowires employed by Kim and Chen *et al.*,[1,12] which had diameters and lengths of about 90–530 nm and 6–8 μm, respectively.

Kim *et al.*[1] found a strong dependence of cell viability on the size of the wires and concluded that the biocompatibility of small diameter nanowires was crucial for the *in situ* study of cellular processes. Instead of relying on the cultured cells to passively subside on the nanowire substrate and allow the penetration of the nanowires,[1] we applied cells to the nanocones with a certain speed to temporarily rupture the cell membranes. The much shallower penetration of the nanocones into the cells would minimize the potential detriment to the cells through piercing all the way through the entire cells. To deliver drug molecules to a high population of cells without endocytosis, methods such as electroporation are most commonly used. Electroporation is used to increase the permeability of the cell plasma membrane by applying an external electrical field. However, this approach often leads to cell death.[13] In contrast, the present intracellular delivery method has overcome such limitations. The enhanced drug delivery into the treated cells was verified by fluorescein staining through flow cytometry.

As a test case, we investigated the nanocone aided intracellular delivery of the cell differentiation reagent to prompt osteoblastic differentiation. It is well established that alkaline phosphatase (ALP) is an important component during hard tissue formation and is a key player in differentiation during early phase development.[14,15] It is hence used as a typical early phase marker during the differentiation in both tissues and bones. The cultured MC-3T3 cells treated with nanocones showed significantly higher ALP activity on the 3rd and 7th days than the control while the activity was lower on the 14th day. This shows that osteoblastic differentiation was enhanced at the early time points after being treated with nanocones, indicating that early bone formation might be potentially promoted.[10] It is highly likely that the enhancement of osteoblastic differentiation in terms of earlier differentiation induction through treatment with nanocones was achieved through facilitating the diffusion of cell differentiation agent molecules into the MC3T3 cells across the cell membranes mechanically disrupted by the sharp diamond nanocones. Our results show that treatment with nanocones is a powerful tool for enhanced transferring of the differentiation medium agent into cells, which can be applied to promote osteoblastic differentiation.

5 Conclusions

A novel type of highly densely packed diamond nanocone array was designed for dramatically enhanced intracellular delivery of drug molecules. The enhanced drug delivery into the treated cells was verified by fluorescein staining through flow cytometry. This technique provides a very simple but yet very effective approach to achieve delivery of molecules to a large number of cells. As a test case, the effect of diamond nanocones on cell differentiation was studied. The present results showed that the mouse MC3T3-E1 pre-osteoblasts treated with a nanocone array had higher differentiation ability at the early stage. This indicates that the nanocones could mechanically disrupt the cell membranes, which aided the delivery of molecules into the cells, but without causing irreversible membrane damage to cells.

Acknowledgements

This study was funded by the City University of Hong Kong (project no. 7200247 and 9667053).

Notes and references

1 W. Kim, J. K. Ng, M. E. Kunitake, B. R. Conklin and P. Yang, *J. Am. Chem. Soc.*, 2007, **129**, 7228.

2 A. K. Shalek, J. T. Robinson, E. S. Karp, J. S. Lee, D.-R. Ahn, M.-H. Yoon, M. Jorgolli, R. S. Gertner, T. S. Gujral, G. MacBeath, E. G. Yang, A. Sutton and H. Park, *Proc. Natl. Acad. Sci. U. S. A.*, 2010, **107**, 1870.
3 A. Schindeler, M. M. McDonald, P. Bokko and D. G. Little, *Semin. Cell Dev. Biol.*, 2008, **19**, 459.
4 P. A. Hill, *British Journal of Orthodontics*, 1998, **25**, 101.
5 V. Lemairea, F. L. Tobina, L. D. Grellera, C. R. Cho and L. J. Suva, *J. Theor. Biol.*, 2004, **229**, 293.
6 D. Khang, J. Choi, Y.-M. Im, Y.-J. Kim, J.-H. Jang, S. S. Kang, T.-H. Nam, J. Song and J.-W. Park, *Biomaterials*, 2012, **33**, 5997.
7 W. T. Codbey and A. Atala, *Ann. N. Y. Acad. Sci.*, 2002, **961**, 10–26.
8 M. Yang, Q. J. Ma, G. T. Dang, K. T. Ma, P. Chen and C. Y. Zhou, *Cytotherapy*, 2005, **7**, 273.
9 H. Ohgushi, N. Kotobuki, H. Funaoka, H. Machida, M. Hirose, Y. Tanaka and Y. Takakura, *Biomaterials*, 2005, **26**, 4654.
10 M. Sila-Asna, A. Bunyaratvej, S. Maeda, H. Kitaguchi and N. Bunyaratavej, *Kobe J. Med. Sci.*, 2007, **53**, 25.
11 C. Wild, R. Kohl, N. Herres, W. Muller-Sebert and P. Koild, *Diamond Relat. Mater.*, 1994, **3**, 373.
12 X. Chen, G. Zhu, Y. Yang, B. L. Wang, L. Yan, K. Y. Zhang, K. K. Lo and W. J. Zhang, *Adv. Healthcare Mater.*, 2013, DOI: 10.1002/adhm.201200362.
13 A. Golberg and B. Rubinsky, *Technol. Cancer Res. Treat.*, 2010, **9**, 423.
14 R. Robison and K. H. Soames, *Biochem. J.*, 1924, **18**, 740.
15 E. E. Golub and K. Boesze-Battaglia, *Curr. Opin. Orthop.*, 2007, **18**, 444.

 This journal is © The Royal Society of Chemistry 2013